Modelling relaxation following T1 transformations of foams incorporating surfactant mass transfer by the Marangoni effect

Ryo Satomi[a], Paul Grassia[a,*], Christophe Oguey[b]

[a] *CEAS, The Mill, University of Manchester, Oxford Road, Manchester M13 9PL, UK*
[b] *LPTM, CNRS UMR 8089, University of Cergy-Pontoise, 2 ave A. Chauvin, 95302 Cergy-Pontoise, France*

Abstract

The dynamics following T1 transformation of foams, during which certain foam films shrink and others grow, was modelled. Variation in surface tension due both to change in surfactant concentration and viscous drag was taken into account. Surfactant transfer was also taken into account, which was assumed to take place between connected films and to be caused by the Marangoni effect. Two models were considered in the first instance, one treating the two sides of shrinking films to be identical and another treating them to be different. Numerical results show plausible behaviours in certain parameter regimes, however with several potential issues. In particular, in one model, singularity was observed above a certain value of the surfactant mass transport coefficient, while such an event was avoided in the other model, as large tension differences between adjacent films are then suppressed. Analysing the results and comparing the models, with a view to applying them to a hexagonal honeycomb foam (rather than just to an isolated set of films), led to a possibility of further improvement; namely incorporating an inter-system surfactant transfer and variation in both surface tension and surfactant concentration along individual films, on top of the mechanisms already considered. Inter-system surfactant transfer was readily incorporated into a third model, which again displayed plausible behaviour.

Keywords:
Foam, T1 topological change, surfactant, Marangoni effect

1. Introduction

Foam is widely applied in different industries such as brewing of beer, oil recovery, pharmaceutical and medical applications [1, 2, 3]. However, due to the topological and geometric complexity of fully 3D foams, mathematical models for 3D foam dynamics tend to be complicated and expensive to implement and visualise [4, 5, 6, 7, 8, 9]. Therefore, in order to reduce complexity to enable simpler modelling, foams confined between two parallel plates separated by a small distance, considered as "2D" foams, have been studied [10, 11, 12, 13, 14, 15, 16, 17, 18, 19, 20, 21, 22, 23, 24, 25, 26, 27].

For 2D foam dynamics, modelling the topological transformation of foams known as T1 transformation has been of significant interest in the research literature [28, 29]. The T1 process is the topological change which can be caused due to imposed strain [30], and it is essentially a switching of neighbouring bubbles, as described in Fig. 1. When foam is strained to the extent where four films meet at a single vertex, the vertex becomes energetically unstable and splits into two threefold vertices [31]. Modelling T1 transformations is also of great practical interest, in particular for sectors involved with microfluidics, such as fine pharmaceutical and biomedical applications [3]. For example, since a T1 transformation involves switching of neighbouring bubbles, obtaining an accurate model of the dynamics of T1 process enables one to control the timing of T1 events [3]: bubble contact time and hence e.g. reaction time in a lab-on-a-chip microfluidic device (where the bubbles might be used to

*Corresponding author
Email addresses: ryo.satomi@gmail.com (Ryo Satomi), paul.grassia@manchester.ac.uk (Paul Grassia), christophe.oguey@u-cergy.fr (Christophe Oguey)

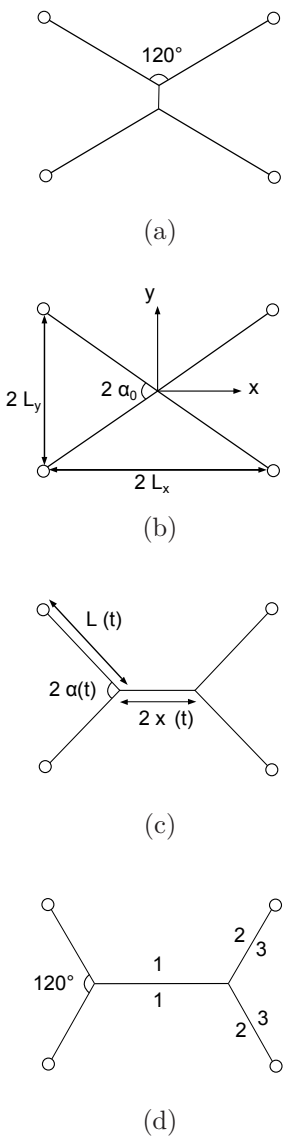

Fig. 1: Structural change that foam films undergo during a T1 transformation. In (a), the vertical film is shrinking due to imposed strain, until it shrinks to the extent where 4 films meet at a single vertex as depicted in (b). A new film is created under the effect of surface tension forces, and its (half)length is denoted by x as shown in (c). In the case where the interfaces on either side of each shrinking film are treated as identical, the newly created film keeps stretching until included angle 2α becomes 120°, as shown in (d). Here (d) also shows the labelling of the interfaces (modulo symmetry).

transport reactants, and where moreover the stability of the film between the bubbles might depend on the T1 [32]) can thereby be precisely controlled. A number of models to simulate foam dynamics have been developed and studied, such as the bubble model, the Potts model, the vertex model and the viscous froth model [10, 14, 16, 29, 33, 34, 35, 36, 37, 38, 39, 40]. However, these existing models are not always suitable to model the T1 transformation dynamics properly (see Embley and Grassia [41]). Some of the major issues include failing to account for appropriate surfactant transfer mechanisms (such as the appropriate mechanisms described in [42]), failure to vary surface tension on foam films with time and not being able to represent the geometry of a (dry) foam accurately: eventually, after a T1, the system should reach an appropriate final state where all films are of roughly comparable lengths and meet at 120° angles.

A model which can potentially resolve some of those issues was devised by Durand and Stone [28], taking varying surface tension into account with a plausible surfactant transfer mechanism. Recently we performed a careful analysis of Durand and Stone's model and its consequences [43]. We discovered that Durand and Stone did not address all of the aforementioned issues such as varying surfactant concentration or surface tension on each and every film, and reaching an appropriate final state. The present work therefore is focused on *modifying* the model by Durand and Stone to address those issues amongst others.

2. Theory

The model by Durand and Stone (which describes film relaxation following T1 transformation of foam) can be interpreted in two different ways. On the one hand, it could be considered to represent 5 isolated films contained in a frame – as e.g. Fig. 1 shows. On the other hand, it could be considered to represent a rectangular unit cell out of a periodic hexagonal honeycomb (in which case the corners of the rectangular unit cell in Fig. 1 represent the midpoints of shrinking films). These two systems are somewhat different, and we focus on the former system in the first instance, returning to the latter system towards the end of the paper.

Fig. 1(c) and (d) show the labelling of the system. Interfaces 1, 2 and 3 refer to the newly created stretching film, the side of shrinking film directly attached to interface 1 and the other side of the shrinking film respectively. Meanwhile x is the (half)length of interface 1, L is the length of interface 2 or 3, and α is half of the angle between the shrinking films. The model is based on the tension balance

$$\gamma_1 = (\gamma_2 + \gamma_3)\cos\alpha \tag{1}$$

where γ_i is the so-called 'total' surface tension of an interface and the subscripts (i = 1, 2, or 3) refer to the

interface labels. The total surface tension γ_i may be expressed as

$$\gamma_i = \gamma_0 - \epsilon \ln \frac{c_i}{c_0} - \frac{\mu}{c_i}\frac{\mathrm{d}c_i}{\mathrm{d}t} \tag{2}$$

where ϵ is the Gibbs elasticity constant, c_i is the surfactant surface concentration (on interface i), t denotes time (so that $\mathrm{d}c_i/\mathrm{d}t$ is the rate of change of surfactant concentration), μ is the surface viscosity and the subscript 0 represents the (initial) equilibrium condition. The first two terms on the right hand side of Eq. (2) represent the static surface tension of an interface given by the Langmuir equation of state [44], and the third term represents the (surface) viscous drag on the interface such that the sum of these gives the total surface tension acting on the interface. Like Durand and Stone we envisage a model for which total surface tension and surfactant concentration are assumed spatially uniform along each interface, but can vary from interface to interface, and also vary with time. Setting $\gamma_2 = \gamma_3 = \gamma_0$ at all times reproduces the Durand and Stone model [28]. Here however we wish to extend beyond Durand and Stone.

Since interfaces 1 and 2 are connected and have different tensions during the T1 process, it is plausible to consider that surfactant is transported between the films by the Marangoni effect. The difference in total tension rather than the static surface tension was assumed to be the driving force and, for simplicity, a linear relationship was assumed so that the transport mechanism may mathematically be expressed as[1]

$$\mathrm{d}(c_1 x)/\mathrm{d}t = D(\gamma_1 - \gamma_2) \tag{3}$$

where D is the empirical Marangoni surfactant mass transfer coefficient[2]. Overall mass conservation demands that

$$\frac{\mathrm{d}}{\mathrm{d}t}(c_1 x) = -\frac{\mathrm{d}}{\mathrm{d}t}(c_2 L)\,. \tag{4}$$

Whilst the true interfilm mass transfer is undoubtedly more complex than Eq. (3) suggests, the model provides a convenient yet plausible theoretical framework within which parametric behaviour of a T1 can be studied.

Initial conditions are imposed as follows. We assume that interfaces are initially at equilibrium surfactant concentration $c_i = c_0$ for each interface ($i = 1$, 2 or 3). This is reasonable provided the process that causes the T1 to occur in the first place (e.g. coarsening and/or imposed strain) is itself inherently much slower than the time scale for the T1 relaxation [45], meaning that T1s tend to occur only intermittently. We can choose the initial value of x to have any small value, much less than the total film length of the system. The smaller the initial value of x, the drier the foam we are attempting to model [45]. The model described above is mathematically well-behaved[3] all the way down to $x \to 0$, so (for simplicity) we chose the initial x to be zero.

With the fundamental mechanisms and conditions mentioned above, two models will be considered in what follows, each representing the '5 films in a frame' situation envisaged in Fig. 1 but with different assumptions on surfactant exchange. In the first model the surfactant concentration on interface 3 will be crudely made equal to that of interface 2, as in the Durand and Stone model (albeit both concentrations will now differ from equilibrium), allowing eventual equality of concentrations on all three interfaces, but necessarily "losing" surfactant to the bulk of the film or the vertex (see [28, 43] for details). This is problematic as surfactant exchange with the bulk should be typically much slower than surfactant mass transport between films by the Marangoni effect. Hence in the second model, conservation of mass on the interface will be regarded as paramount, i.e. surfactant on interface 3 cannot exchange mass with the bulk, leading to treating interfaces 2 and 3 differently. The models referred to above will be named model 1 and model 2 respectively. Subsequently we will attempt to adapt the models for the T1 from the '5 isolated films in a frame' to the case of a periodic honeycomb structure. This requires surfactant transfer between interface 2 and an attached periodic copy of interface 3. This will lead to consideration of a third model, named model 3.

[1] Some support for a mass transfer relation of this type can be obtained by appealing to fluid mechanical arguments matching the Marangoni stress to the viscous shear stress at film surfaces associated with velocity gradients across the film thickness in the presence of bulk film viscosity.

[2] It is not possible for Eq. (3) to replicate Durand and Stone's model with any constant value of D, but the model can be replicated by allowing D to evolve in a very specific (albeit somewhat artificial) way over time. Initially D must be very small – because the surfactant mass transport rate in Durand and Stone is tied to the growth rate in film length, which scales at first with the initial film length itself. However the growth rate of film length then undergoes a dramatic increase – even whilst the film is quite short [43]: the dimensionless D peaks at a value between 2–3 (depending on the ϵ value). Subsequently D decreases, and indeed, for any finite ϵ, the final D must vanish (this is the only way to sustain unequal surfactant concentrations assumed in Durand and Stone's final state).

[3] This good behaviour in the $x \to 0$ limit is a contrast from Durand and Stone's original model [28]. If x is initially zero in that model, then x remains identically zero for a well-defined, finite time, after which it begins to grow at a finite rate [43]. In order to avoid this non-smooth behaviour, the initial x was chosen to have a small but finite value in the analysis of the Durand and Stone model [43]

3. Results and discussion

Eqs. (1)–(3) constitute a set of ordinary differential equations for film lengths and film surfactant concentrations that can be readily solved numerically – we used the built-in numerical differential equation solver from the commercial software Mathematica. The variables in the governing equations were normalised[4] in such a way that γ_0, c_0 and μ are all unity, whilst $L_x = \sqrt{3}$ and $L_y = 1$ with non-dimensional units (see Fig. 1(b) for definitions of L_x and L_y). Parametric studies in the dimensionless analogues of ϵ and D (which, for economy of notation, we continue to denote by the original symbols ϵ and D) were then carried out for the two models. Literature [28] suggests that the dimensionless ϵ can be up to order unity, but for certain surfactants it may be permitted to adopt values which are much smaller [30]. First principles estimates of the dimensionless D are difficult to obtain – depending on the estimation procedure one adopts, values can be obtained that are much smaller than unity or much larger than unity (see appendix). In what follows, numerical results of the various models will first be discussed individually, based on which a comparison and a general discussion will follow.

3.1. Model 1: treating interfaces 2 and 3 as identical

Fig. 2 shows some of the results produced by model 1, assuming ϵ=1 and either D=1 or D=5. Both film lengths and concentrations evolve in plausible ways. Interface 1 stretches and interface 2 shrinks to attain the equal angles between all films in the final state. Initial rapid decrease in c_1 (the surfactant coverage on interface 1) is observed, followed by a gradual increase to the final value. The initial rapid decrease in concentration is due to mechanical relaxation (stretch) taking place faster than surfactant can migrate from interface 2. After approaching the final film length, mechanical relaxation ceases and surfactant transfer due to physico-chemical relaxation (i.e. Marangoni driven surfactant flux) becomes the dominant process, observed as the gradual increase in c_1. Meanwhile, at least for the case $D = 1$, c_2 (the surfactant coverage on interface 2) generally evolves in an analogous manner; that is, the concentration increases due to rapid shrinkage, then decreases gradually due to surfactant transfer.

[4]Our non-dimensionalisations correspond to dividing lengths by the (dimensional) distance L_y, dividing film tensions by γ_0, dividing surfactant surface coverages by c_0, and dividing time by μ/γ_0. The dimensionless analogue of ϵ is obtained by dividing the dimensional ϵ by the value γ_0. The dimensionless analogue of D is obtained by dividing the dimensional D by the factor $c_0 L_y/\mu$.

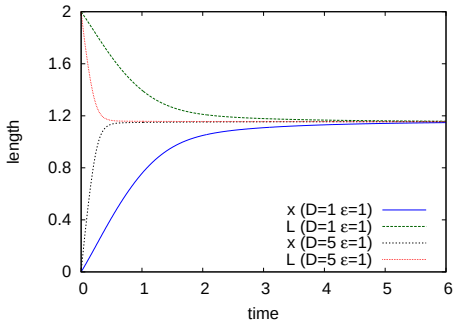

(a)

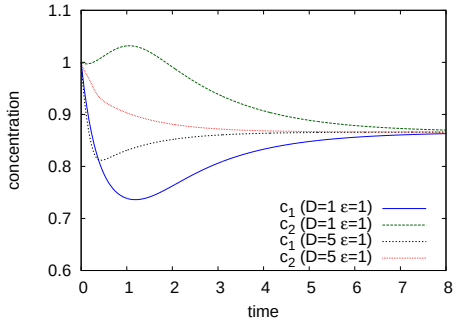

(b)

Fig. 2: Evolution with time of the T1 process in model 1. The y-axis corresponds to length and concentration for (a) and (b) respectively. Lengths, times and concentrations are all non-dimensionalised here.

As D is increased, say from D=1 to D=5, surfactant transport becomes more sensitive to the tension difference so that physico-chemical relaxation takes place faster. This is evidenced by the absence of initial increase in c_2 as it can be interpreted that surfactant migrates from interface 2 to interface 1 faster than it builds up due to mechanical shrinkage, as can be seen in Fig. 2(b). However this transferred material facilitates the shortening of interface 2 and the lengthening of interface 1, with the result that mechanical relaxation also takes place faster.

The model fails above a critical value of D (≈ 18.3 for both the values $\epsilon = 0$ and $\epsilon = 1$) in which case the model becomes singular and cannot be solved (as a proper single valued function $x(t)$). In fact, the model predicts unrealistic behaviour of near-instantaneous jumps in both film length and concentration with D close to the critical value. Physically, this catastrophic behaviour of the system can be considered as follows. A large value of D leads to a high mass transfer rate i.e. large value of $\mathrm{d}(c_1 x)/\mathrm{d}t$ in Eq. (3). High mass transfer rate leads to rapid change in c_1 and x by $\mathrm{d}(c_1 x)/\mathrm{d}t = x\mathrm{d}c_1/\mathrm{d}t +$

$c_1 \mathrm{d}x/\mathrm{d}t$. The rapid change in c_1 leads to higher surface tension, in particular a strong surface viscous contribution to the total surface tension, by Eq. (2). Higher surface tension leads to an even higher mass transfer rate and thus the system evolves catastrophically. In reality however, such fast catastrophic evolution is unlikely to be observed, so there must be a flaw within the model. To the extent that a model treating surface tensions and surface concentrations as spatially uniform along individual films is reasonable, one way to avoid this predicted catastrophic behaviour may be that the empirical mass transfer coefficient D experimentally never attains such large values. Alternatively, the problem may be that the tensions in interfaces 2 and 3 actually differ, which is the situation considered in Section 3.2.

3.2. *Model 2: treating interfaces 2 and 3 as evolving differently*

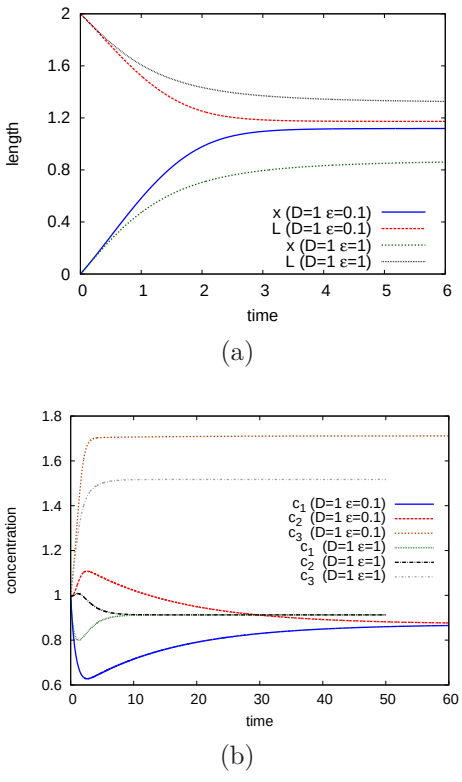

Fig. 3: Evolution with time of the T1 process in model 2. The y-axis corresponds to lengths and concentrations in (a) and (b) respectively. Lengths, times and concentrations are all non-dimensionalised here.

Fig. 3 shows some of the numerical results produced by model 2. Since interface 3 is, in model 2, isolated from interfaces 1 and 2, it can be observed in Fig. 3(b) that c_3 does not attain the same final concentration as c_1 and c_2, at least on time scales short compared to the time required to diffuse surfactant *across* films between surfaces and film interiors. As a consequence, the various films have different tensions in the final state, similarly to the original Durand and Stone model. Hence films meet at unequal angles to satisfy the tension balance, as can be inferred from Fig. 3(a). As evidenced in Fig. 3(a), increasing ϵ causes the final x to decrease, i.e. the final state structure diverges from a fully chemically equilibrated structure (films meeting at 120°) with increasing ϵ. This is plausible, since a larger value of ϵ means the tension is more sensitive to concentration, so that γ_3 decreases relative to γ_1 and γ_2 which in turn results in greater deviation from the equal angle state.

As the value of D is increased, the system evolves faster in a similar way to model 1, but remarkably a critical catastrophic value of D does not exist under any conditions in model 2. This may be attributed to the force balance of model 2. When surfactant flux is very sensitive to surface tension difference due to large value of D, the system arranges itself such that surface tensions γ_1 and γ_2 are nearly the same, keeping surfactant flux finite and thus avoiding a catastrophic behaviour. This is possible with model 2 because the force balance Eq. (1) may still be satisfied owing to the fact that γ_3 can, unlike in model 1 (where necessarily $\gamma_3 = \gamma_2$), be significantly less than either γ_1 or γ_2. Indeed a significant drop in γ_3 has been found to occur (data are not shown here) due to rapid shrinkage of interface 3 leading also to rapid increase in c_3.

3.3. *Comparison of models 1 and 2*

From the individual results, it is clear that the main differences between the two models are in the final state and in the presence or absence of the critical value of D. Geometrically, the final state achieved by model 1 is evidently more symmetric than that by model 2 as it achieves equal film angles. However, the final concentration is lower than the concentration at the initial instant when the T1 transformation starts: the concentrations at the initial instant can only be recovered by invoking another surfactant transport mechanism (e.g. surfactant exchange between film surface and bulk). This lower concentration in the final state is due to the fact that the total film length on which surfactant is conserved (i.e. $x + L$) of the final state is longer than that of the initial state, and the concentration of surfactant on interface 3 (in model 1) is forced to be equal to that of interface 2. Thus, even though model 1 allows the system to reach a final state geometrically equivalent to full chemical equilibration, it is still incomplete in regards of the evolution of concentration of surfactant.

Model 2 does not itself attain a final state with equal film angles. However, the modelled dynamics is plausible (avoiding catastrophe for any chosen D) suggesting that treating interfaces 2 and 3 differently is crucial in order to model film dynamics accurately. There may be ways in which catastrophe can be avoided in model 1 also: e.g. restricting the permitted values of D, and/or allowing D to be time-dependent, and/or switching to a nonlinear relationship between surfactant flux and tension in lieu of Eq. (3) and/or recognising that tensions actually vary spatially along interfaces and not merely between one interface and the next. However switching to model 2 appears far more straightforward, further supporting the idea that interfaces 2 and 3 should be treated differently.

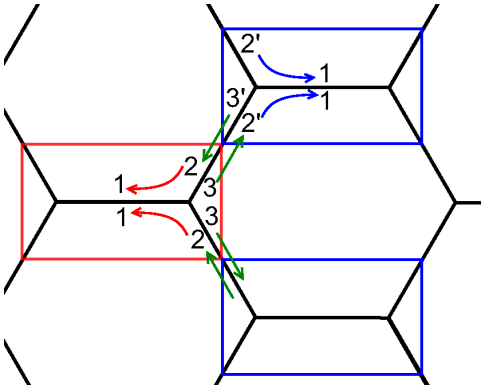

Fig. 4: A periodically replicated system producing a hexagonal honeycomb structure. As shown, such a structure can be constructed by joining copies of the '5 film' system considered in this work.

Based on the above comparison, it is worth speculating whether the 5 film approach used in this work, as shown in Fig. 1, can be modified to the case of a periodic honeycomb structure shown in Fig. 4 undergoing a T1 process under applied strain, and indeed whether an improved version of the model may be posed. First on symmetry grounds, the Plateau state (120° film meeting angles) still must be attained when modelling the periodic honeycomb structure as it clearly is the true final state for this particular system, but this must be achieved without artificially losing mass from interface 3 (an issue with model 1). The only way to do so is by considering surfactant flow in and out of each 'unit cell' of the system. Fig. 4 shows a periodic honeycomb structure represented by multiple '5 film unit cells' systems joined together. Since interface 3 is connected to a copy of interface 2 in the neighbouring unit cell (interface 2′) and likewise interface 2 connects to a copy of interface 3 denoted interface 3′, any inequality in concentrations at the connection point will induce a Marangoni flow tending to oppose that concentration inequality.

A simple special case arises when surfactant transport across the connection point between interfaces 2 and 3′ is assumed to be far more efficient than that between interfaces 1 and 2. One then obtains a model where total tension is uniform along the entire length $2L$ of the joint interface 2-3′, i.e. $\gamma_3 = \gamma_2$ (and also $c_3 = c_2$). We refer to this situation as model 3, and analyse it in the next section.

3.4. *Model 3: a model for relaxation of a periodic honeycomb structure*

Mathematically the equations governing model 3 are very similar to those for model 1, except that the surfactant conservation equation is now

$$\frac{\mathrm{d}}{\mathrm{d}t}(c_1 x) = -2\frac{\mathrm{d}}{\mathrm{d}t}(c_2 L)\,. \tag{5}$$

in lieu of Eq. (4). This apparently minor change reflects the fact that for a periodic honeycomb structure there is surfactant flux across geometrically fixed symmetry points, while there are also points with no flux across them, which are not geometrically fixed (see Fig. 5).

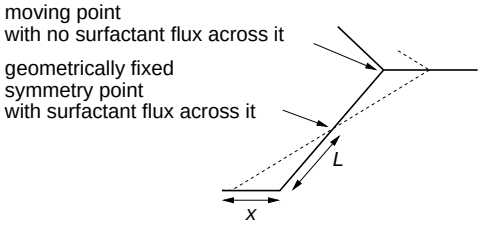

Fig. 5: Segment of a relaxing honeycomb at a given instant in time, showing the geometrically fixed symmetry point and also the point which surfactant (located on the left hand interfaces of the films which join together there) cannot cross. The dashed lines show the configuration at an earlier point in time.

Results for model 3 are shown in Fig. 6. Model 3 reaches (like model 1) a final state which is a Plateau state (120° angles). However final concentrations on films (denoted c_1 and c_2) are now higher (not lower) than the equilibrium concentration (again see Fig. 6). This is because surfactant now spreads over a total film length $x+2L$, and this decreases as x increases, whereas $x+L$ (the length accessible to surfactant on interfaces 1 and 2 in model 1) increases with increasing x.

Model 3 (like model 2, but unlike model 1) also does not exhibit any critical or catastrophic behaviour as D increases. Instead, in the very large D limit, Eqs. (1)–(3) can be satisfied by making γ_1 and γ_2 become small

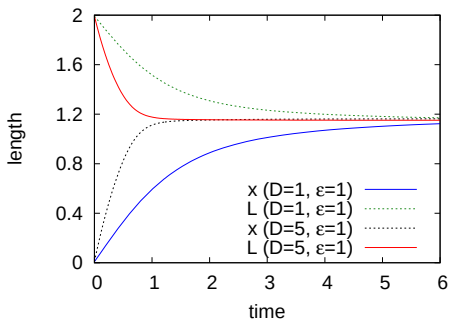

(a)

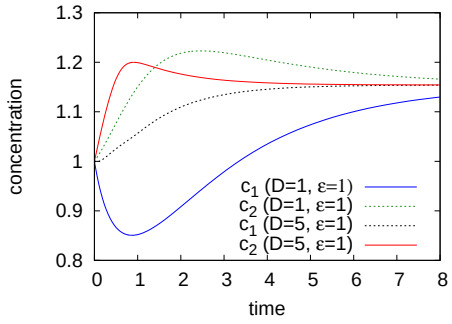

(b)

Fig. 6: Evolution with time of the T1 process for (a) lengths and (b) concentrations, according to model 3.

quantities, with $\gamma_3 = \gamma_2$ always in model 3: in dimensionless terms γ_1 and γ_2 each become $O(1/D)$, but necessarily remain unequal, as otherwise Eq. (1) would be violated except in the Plateau state. This requires that the surface viscous term in each case nearly cancels the static tension, and moreover that interface 1 is sufficiently strongly coupled to interface 2-3′ that material elements on all interfaces 1, 2 and 3′ shrink at nearly the same rate.

The reason why such a solution for large D is admissible in the case of model 3, but not in the case of model 1, is connected to the above observation that $x + 2L$ is a decreasing function of x, whereas $x + L$ is an increasing function of x. Static surface tension can only be cancelled by surface viscosity when film material elements are shrinking, never when they are stretching. For model 3, the total available length of film $x + 2L$ shrinks as x grows, whereas for model 1, the only way to decrease the total available length of film $x + L$ is to decrease x: decreasing x, however, immediately 'undoes' the T1 transformation.

3.5. Shear across film thicknesses

We have seen in the previous section that model 3 has a number of attractive features for describing the relaxation of the periodic honeycomb structure: it attains a Plateau final state (unlike model 2), it does not lose any net surfactant mass from interfaces (unlike model 1) and behaves plausibly even in the limit of large mass transfer coefficients between films (again unlike model 1).

There is however an important outstanding issue with the model as it currently stands. The velocity of a material element at any arbitrary point along interface 2 differs from the velocity of the material element directly opposite on interface 3: in other words there is shear across the thickness of the film[5]. Since the liquid in the film has a finite (bulk) viscosity, a shear stress results. This shear stress can only be supported by a gradient in total tension along the film. Although it is possible to envisage a situation in which the spatial changes in total tension along any given film are negligible compared to the tension change between that film and its neighbours, such a situation is somewhat contrived: a model that properly addresses continuous spatial variations in tensions along films is desirable. Such a model will however be considerably more numerically expensive than any of those which have been considered here.

4. Conclusions

The model of the T1 process presented in this work yielded results plausible in many aspects, addressing to a certain extent the physics missing from previous existing models such as time-varying surfactant concentrations and incorporating inter-film surfactant transfer due to the Marangoni effect. However, the introduction of a new surfactant transfer mechanism and time-varying surface tension gave rise to further complications and associated problems such as the appearance of a critical value of the surfactant mass transfer coefficient D beyond which catastrophic film growth is predicted (model 1). These issues however may be addressed by further modifying the model to account e.g. for different surfactant concentrations on different sides of a given film and/or surfactant exchange between periodic copies of the system undergoing the T1. Which mechanisms need to be incorporated in models depends on the physical system being considered: an isolated system

[5] Shear also arises with model 2, but the situation is less acute than in model 3: in the case of model 2 (which purports to describe an isolated system of 5 films in a frame), the shear vanishes at the pegged endpoint of the shrinking film.

of 5 films in a frame (model 2) should behave differently from a periodic array of hexagons (model 3). Although the T1 evolution process proposed here seems reasonable, experimental results are also desired in order to test the validity of the model and estimate suitable values of the empirical mass transfer coefficient D (see also the appendix). Experimental results may also clarify the extent to which models which treat individual interfaces as spatially uniform entities are appropriate, or whether consideration of spatial variation (of tensions and/or surfactant concentrations) within interfaces is essential.

Appendix A. Estimation of mass transfer coefficient

Here an attempt is made to estimate the magnitude of the surfactant mass transfer coefficient. The surfactant mass transfer could be driven by two factors: a diffusive effect or a Marangoni effect, whose driving force would be respectively the difference in static surface tensions (associated with a difference in surfactant concentrations) or the difference in total tensions on connected films. We denote the associated mass transfer coefficients as D_{diff} and D_{mar} respectively.

If the mass transfer is diffusively driven across a vertex, then the mass transfer rate would be $\mathcal{D}_{\text{mol}}(c_2 - c_1)/l$ where $\mathcal{D}_{\text{mol}}$ is the molecular diffusivity (typical order of magnitude 10^{-9} m^2 s^{-1}), c_1 and c_2 are surfactant concentrations, and l is the distance over which the difference in surfactant concentrations is realised. If the concentration change is assumed to be localised where films meet at a vertex, then l is simply the vertex size (physically the tricuspid triangular 'vertex' could be up to about 1 mm in size, but possibly substantially smaller when the foam is very dry). The difference in static surface tensions (for weak departures from the equilibrium concentration c_0) would be roughly $\epsilon(c_2 - c_1)/c_0$ (see Eq. (2) in the main text), with the result that

$$D_{\text{diff}} \approx \frac{\mathcal{D}_{\text{mol}} c_0}{\epsilon l} \tag{A.1}$$

where a definition analogous to Eq. (3) has been used.

The dimensionless analogue follows (as in the main text) by scaling lengths by L_y, tensions by γ_0, concentrations by c_0, and times by μ/γ_0. The dimensionless mass transfer coefficient which will be denoted here as $\bar{D}_{\text{diff}}$ (to distinguish it from its dimensional analogue) can be estimated to be

$$\bar{D}_{\text{diff}} \approx \frac{\mu}{\epsilon} \frac{\mathcal{D}_{\text{mol}}}{L_y l}. \tag{A.2}$$

A system length scale L_y (up to about 1 cm) was chosen as a typical value. We employed the values of $\mathcal{D}_{\text{mol}}$ and l suggested above, and took μ and ϵ values of the same order of magnitude as reported by Durand and Stone [28], e.g. around 1 mPa m s and 30 mN m^{-1} respectively.

Adopting Eq. (A.2), $\bar{D}_{\text{diff}}$ is predicted to be about 3×10^{-6} typically. For a drier foam (e.g. a 10 fold decrease in l), with smaller bubbles (e.g. a 3 fold decrease in L_y) and with a high surface viscosity surfactant such as bovine albumin (a roughly 30 fold increase in μ according to Durand and Stone [28] compared to the surfactant SDS) it may rise up to about 3×10^{-3} but it is still a small parameter for a diffusive drive.

Clearly molecular diffusion is very inefficient at moving surfactant along films on the time scales of interest for a T1 transformation, so that a convective mechanism (see e.g. [46, 47, 48, 49]) needs to be invoked to transport surfactant from film to film. Adopting full tension as the driving force for the Marangoni convection yields a different estimate for the mass transfer coefficient D_{mar}. First, it can be estimated that

$$\frac{\gamma_1 - \gamma_2}{l} \approx \mu_b \frac{u_{\text{mar}}}{h} \tag{A.3}$$

where $\gamma_1 - \gamma_2$ is the change in full tensions of the two connected interfaces (interfaces 1 and 2; a typical tension difference of up to 30 mN m^{-1} in an extreme case where a growing film becomes depleted in surfactant and a shrinking film becomes covered with surfactant), μ_b is the bulk viscosity (1 mPa s for an aqueous system), u_{mar} is the (a priori unknown) Marangoni velocity and h is the thickness across which the Marangoni flow produces shear (which would be the vertex thickness in the system adopted in this work where the Marangoni stresses localise on vertices, but could be substantially smaller in a continuum model where Marangoni flows exists on films as well; see Fig. 7). As previously, l denotes the length scale along the surface over which the total tension changes. In the system considered in this work it is the size of a vertex, since surface tension only changes between films. However the 'effective' l would be substantially larger were we to consider a continuum model where full tension changes all the way along a film (again see Fig. 7).[6] For the typical parameter values mentioned above, $u_{\text{mar}} \approx 30$ m s^{-1} $\times (h/l)$ where (h/l) is order unity for the system considered in this work or any other 'change localised at vertices' type model, but

[6] In a continuum model, local Marangoni fluxes would of course depend on local gradients of full tension. We could however *define* the parameter l as the difference between spatial averages of full tensions on interfaces 1 and 2, divided by the gradient of full tension at the point where those interfaces meet. The resulting length scale would be comparable with film lengths.

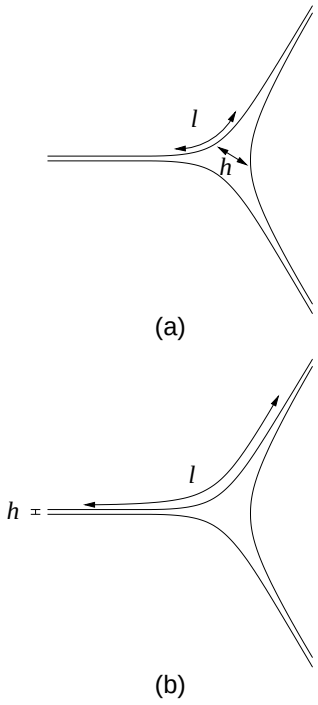

Fig. 7: Zoomed view of a vertex and the films to which it attaches. Very different values for the 'thickness to length' ratio h/l are obtained depending upon whether the focus is on (a) the vertex itself or (b) on the films.

is tiny compared to unity otherwise. It is also plausible that h/l could be time-dependent: tension changes might be localised near vertices initially, but then spread out over longer distances to regions where film thicknesses are lower.

The Marangoni surfactant flux can be estimated simply as $u_{\rm mar}c_0$, leading to an estimate (via Eqs. (3) and (A.3))

$$D_{\rm mar} \approx \frac{c_0}{\mu_b}\frac{h}{l} \qquad \text{(A.4)}$$

and hence a dimensionless analogue (denoted here by $\bar{D}_{\rm mar}$)

$$\bar{D}_{\rm mar} \approx \frac{\mu}{\mu_b L_y}\frac{h}{l}. \qquad \text{(A.5)}$$

Here $\mu/(\mu_b L_y)$ can be considered as a reciprocal of surface mobility parameter. Choosing values as above (μ = 1 mPa m s and μ_b = 1 mPa s and L_y =10^{-2} m), this quantity would typically be about 100, giving

$$\bar{D}_{\rm mar} \approx 100\frac{h}{l}. \qquad \text{(A.6)}$$

Thus the value of $\bar{D}_{\rm mar}$ depends crucially on the ratio of the length scales, namely the thickness scale and the longitudinal scale, h/l.

For models where tension changes are localised at vertices, the factor h/l is order unity, so $\bar{D}_{\rm mar}$ could be as large as 100, well above the critical value observed for model 1 in this work. However for models in which tensions vary continuously along films (rather than being localised at vertices) the relevant value of h/l and hence of $\bar{D}_{\rm mar}$ will be many times smaller (and the values of 1 and 5 adopted in Fig.s 2, 3 and 6 are therefore plausible). Exploring the parametric behaviour of the models presented in the main text over a broad range of possible surfactant mass transfer coefficients is therefore of interest.

List of symbols employed in the main text

c_i	surfactant concentration on interface i
D	mass transfer coefficient
L	length of shrinking film
L_x, L_y	length scales of rectangle enclosing T1
x	(half)length of growing film
t	time
$_0$	the subscript denotes equilibrium values
α	half of angle made by the shrinking films
ϵ	Gibbs elasticity constant
γ_i	total surface tension on interface i
μ	surface viscosity

List of additional symbols employed in the appendix

$\mathcal{D}_{\rm mol}$	molecular diffusivity
l	length scale along vertex or film
h	lhickness scale across vertex or film
$u_{\rm mar}$	Marangoni velocity
$\bar{}$	overbar denotes a dimensionless quantity
$_{\rm diff}$	subscript denotes a diffusive mechanism
$_{\rm mar}$	subscript denotes a Marangoni mechanism
μ_b	bulk viscosity

References

[1] A. M. Kraynik. Foam flows. *Annu. Rev. Fluid Mech.*, 20:325–357, 1988.

[2] J. P. Heller and M. S. Kuntamukkula. Critical review of the foam rheology literature. *Ind. Eng. Chem. Res.*, 26:318–325, 1987.

[3] W. Drenckhan, S. J. Cox, G. Delaney, H. Holste, D. Weaire, and N. Kern. Rheology of ordered foams—on the way to discrete microfluidics. *Colloids Surf., A*, 263:52–64, 2005.

[4] A. M. Kraynik, D. A. Reinelt, and F. van Swol. Structure of random monodisperse foam. *Phys. Rev. E*, 67:031403, 2003.

[5] D. A. Reinelt and A. M. Kraynik. Simple shearing flow of dry soap films with tetrahedrally close packed structure. *J. Rheol.*, 44:453–471, 2000.

[6] D. Reinelt, P. Boltenhagen, and N. Rivier. Deformed foam structure and transitions in a tube. *Eur. Phys. J. E*, 4:299–304, 2001.

[7] D. A. Reinelt and A. M. Kraynik. Simple shearing flow of a dry Kelvin soap foam. *J. Fluid Mech.*, 311:327–342, 1996.

[8] D. A. Reinelt and A. M. Kraynik. Large elastic deformations of 3-dimensional foams and highly concentrated emulsions. *J. Colloid & Interf. Sci.*, 159:460–470, 1993.

[9] D. Weaire and R. Phelan. A counter-example to Kelvin's conjecture on minimal surfaces. *Phil. Mag. Lett.*, 69:107–110, 1994.

[10] T. E. Green, P. Grassia, L. Lue, and B. Embley. Viscous froth model for a bubble staircase structure under rapid applied shear: an analysis of fast flowing foam. *Colloids Surf., A*, 348:49–58, 2009.

[11] T. E. Green, A. Bramley, L. Lue, and P. Grassia. Viscous froth lens. *Phys. Rev. E*, 74:051403, 2006.

[12] P. Grassia, G. Montes-Atenas, L. Lue, and T. Green. A foam film propagating in a confined geometry: analysis via the viscous froth model. *Eur. Phys. J. E*, 25:39–49, 2008.

[13] I. Cantat. Gibbs elasticity effect in foam shear flows: a non quasi-static 2d numerical simulation. *Soft Matter*, 7:448–455, 2011.

[14] I. Cantat and R. Delannay. Dissipative flows of 2d foams. *Eur. Phys. J. E*, 18:55–67, 2005.

[15] I. Cantat and R. Delannay. Dynamical transition induced by large bubbles in two-dimensional foam flows. *Phys. Rev. E*, 67:031501, 2003.

[16] S. J. Cox. A viscous froth model for dry foams in the Surface Evolver. *Colloids Surf., A*, 263:81–89, 2005.

[17] S. Cox, D. Weaire, and J. A. Glazier. The rheology of two-dimensional foams. *Rheol. Acta*, 43:442–448, 2004.

[18] T. Okuzono and K. Kawasaki. Intermittent flow behaviour of random foams: a computer experiment on foam rheology. *Phys. Rev. E*, 51:1246–1253, 1995.

[19] T. Okuzono, K. Kawasaki, and T. Nagai. Rheology of random foams. *J. Rheol.*, 37:571–586, 1993.

[20] S. A. Khan and R. C. Armstrong. Rheology of foams. II. Effects of polydispersity and liquid viscosity for foams having gas fraction approaching unity. *J. non-Newtonian Fluid Mech.*, 25:61–92, 1987.

[21] S. A. Khan and R. C. Armstrong. Rheology of foams. I. Theory for dry foams. *J. non-Newtonian Fluid Mech.*, 22:1–22, 1986.

[22] A. M. Kraynik and M. G. Hansen. Foam rheology: a model of viscous phenomena. *J. Rheol.*, 31:175–205, 1987.

[23] A. M. Kraynik and M. G. Hansen. Foam and emulsion rheology: a quasistatic model for large deformations of spatially periodic cells. *J. Rheol.*, 30:409–439, 1986.

[24] H. M. Princen and A. D. Kiss. Rheology of foams and highly concentrated emulsions. III. Static shear modulus. *J. Colloid & Interf. Sci.*, 112:427–437, 1986.

[25] H. M. Princen. Rheology of foams and highly concentrated emulsions. I. Elastic properties and yield stress of a cylindrical model system. *J. Colloid & Interf. Sci.*, 91:160–175, 1983.

[26] D. Weaire and J. P. Kermode. Computer simulation of a 2-d soap froth. II. Analysis of results. *Phil. Mag. B*, 50:379–395, 1984.

[27] D. Weaire and J. P. Kermode. Computer simulation of a 2-d soap froth. I. Method and motivation. *Phil. Mag. B*, 48:245–259, 1983.

[28] M. Durand and H. A. Stone. Relaxation time of the topological T1 process in a two-dimensional foam. *Phys. Rev. Lett.*, 97:226101, 2006.

[29] N. Kern, D. Weaire, A. Martin, S. Hutzler, and S. J. Cox. Two-dimensional viscous froth model for foam dynamics. *Phys. Rev. E.*, 70:041411, 2004.

[30] A.-L. Biance, S. Cohen-Addad, and R. Höhler. Topological transition dynamics in a strained bubble cluster. *Soft Matter*, 5:4672–4679, 2009.

[31] D. Weaire and S. Hutzler. *The Physics of Foams*. Oxford University Press, 1999.

[32] A.-L. Biance, A. Delbos, and O. Pitois. How topological rearrangements and liquid fraction control liquid foam stability. *Phys. Rev. Lett.*, 106:068301, 2011.

[33] D. J. Durian. Foam mechanics at the bubble scale. *Phys. Rev. Lett.*, 75:4780–4783, 1995.

[34] D. J. Durian. Bubble-scale model of foam mechanics: Melting, nonlinear behaviour and avalanches. *Phys. Rev. E*, 55:1739–1751, 1997.

[35] Y. Jiang, P. J. Swart, A. Saxena, M. Asipauskas, and J. A. Glazier. Hysteresis and avalanches in two-dimensional foam rheology simulations. *Phys. Rev. E*, 59:5819–5832, 1999.

[36] S. Sanyal and J. A. Glazier. Viscous instabilities in flowing foams: a cellular Potts model approach. *J. Stat. Mech.: Theory & Exper.*, 2006:P10008, 2006.

[37] G. L Thomas, J. C. M. Mombach, M. A. P. Idiart, C. Quilliet, and F. Graner. Simulations of viscous shape relaxation in shuffled foam clusters. *Colloids Surf., A*, 263:90–94, 2005.

[38] C. Raufaste, B. Dollet, S. Cox, Y. Jiang, and F. Graner. Yield drag in a two-dimensional foam flow around a circular obstacle: Effect of liquid fraction. *Eur. Phys. J. E*, 23:217–228, 2007.

[39] S. A. Jones, B. Dollet, N. Slosse, Y. Jiang, S. J. Cox, and F. Graner. Two-dimensional constriction flows of foams. *Colloids Surf., A*, 382:18–23, 2011.

[40] T. Okuzono and K. Kawasaki. Intermittent flow behavior of random foams: a computer experiment on foam rheology. *Phys. Rev. E.*, 51:1246–1253, 1995.

[41] B. Embley and P. Grassia. Viscous froth simulations with surfactant mass transfer and Marangoni effects: deviation from Plateau's rules. *Colloids Surf., A*, 382:8–17, 2011.

[42] D. A. Edwards, H. Brenner, and D. T. Wasan. *Interfacial Transport Processes and Rheology*. Butterworth-Heinemann, London, 1991.

[43] P. Grassia, C. Oguey, and R. Satomi. Relaxation of the topological T1 process in a two-dimensional foam. *Eur. Phys. J. E*, 35:64, 2012.

[44] E. H. Lucassen-Reynders, A. Cagna, and J. Lucassen. Gibbs elasticity, surface dilational modulus and diffusional relaxation in nonionic surfactant monolayers. *Colloids Surf., A*, 186:63–72, 2001.

[45] P. Grassia, B. Embley, and C. Oguey. A Princen honeycomb foam out of physicochemical equilibrium. *J. Rheol.*, 56:501–526, 2012.

[46] B. N. Hewakandamby and W. B. Zimmerman. Characterisation of hydraulic jumps/falls with surface tension variations in thin film flows. *Dynam. Atmos. Oceans*, 34:349–364, 2001.

[47] W. B. Zimmerman, J. M. Rees, and B. N. Hewakandamby. Numerical analysis of solutocapillary Marangoni-induced interfacial waves. *Adv. Colloid Interface Sci.*, 134–135:346–359, 2007.

[48] M. Roché, Z. Li, I. Griffiths, A. Saint-Jalmes, and H. A. Stone. Surfactant-assisted spreading of an oil-in-water emulsion on a liquid bath, 2010. arXiv:1010.3236v1.

[49] A. Saint-Jalmes, M. Roché, Z. Li, I. M. Griffiths, and H. A. Stone. Surfactant spreading on water: the 'capillary jump' (Plenary lecture). In *9th European Conference on Foams, Emulsions and Applications, EUFOAM 2012, Lisbon, Portugal, 8–11 July*, 2012.